test. A capacitor was placed across the output of the dc power supply to decrease the potential of damaging the dc power supply with the high ripple currents generated during testing.

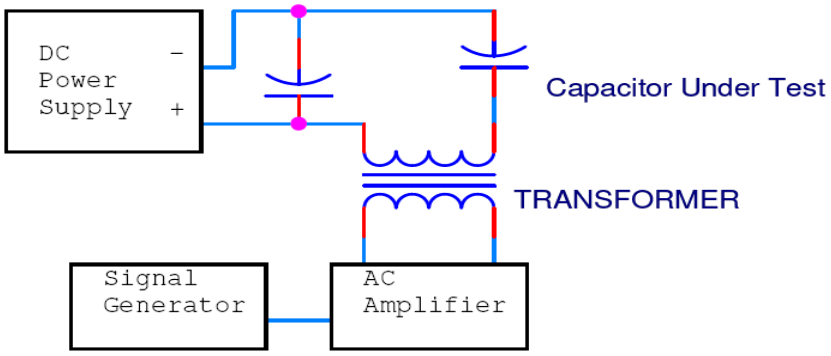

Fig. 2.33. Ripple current test schematic.

Thermocouples (TCs) were applied to the module in the center of both sides as shown in Fig. 2.34. Ripple current was applied in 50 A steps starting at 100 A and stopping at 250 A [root mean square (rms)]. The temperature was allowed to stabilize for 30 minutes before data was recorded. The two TC temperatures were averaged and plotted to determine the module's temperature response to high ripple current values. These data are shown in Fig. 2.35, which shows that the average temperature rise from 0–250 A was 11°C for the Camry capacitor module. The data for the 7.5 kHz test stopped at 190 A due to the limitations of the alternating current (ac) amplifiers. Nonetheless, the test results indicate that the Camry is capable of withstanding high ripple currents without reaching excessive temperatures. Results from dynamic tests upon the Prius module at 4 kHz are provided in Fig. 2.36, and indicate that the steady state temperature of the Prius module with a 200 A ripple current is about 52°C, whereas the steady state temperature of the Camry module with a 200 A ripple current at 5 kHz is only 28°C.

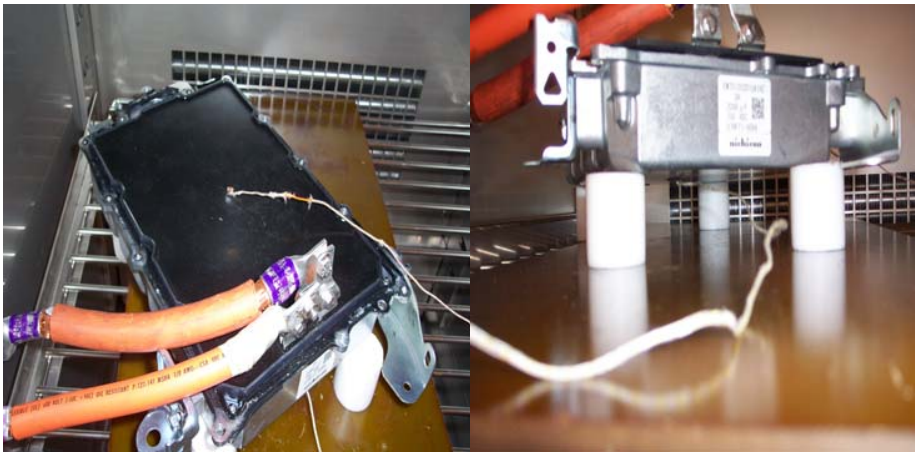

Fig. 2.34. TCs on the Camry capacitor module.

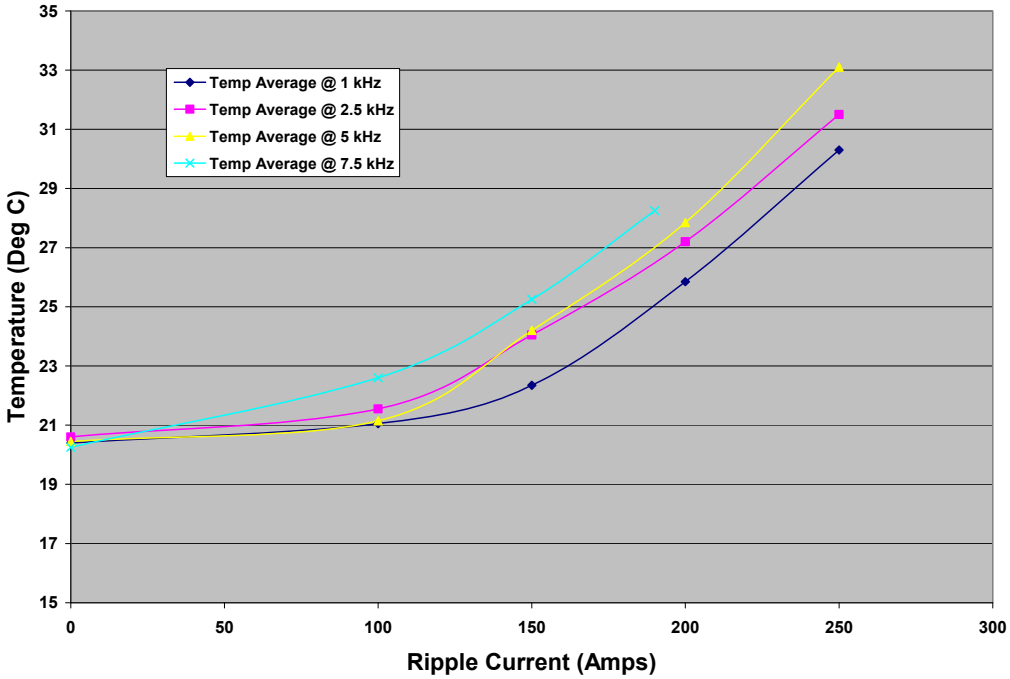

Fig. 2.35. Camry capacitor module steady-state temperature response vs. ripple current.

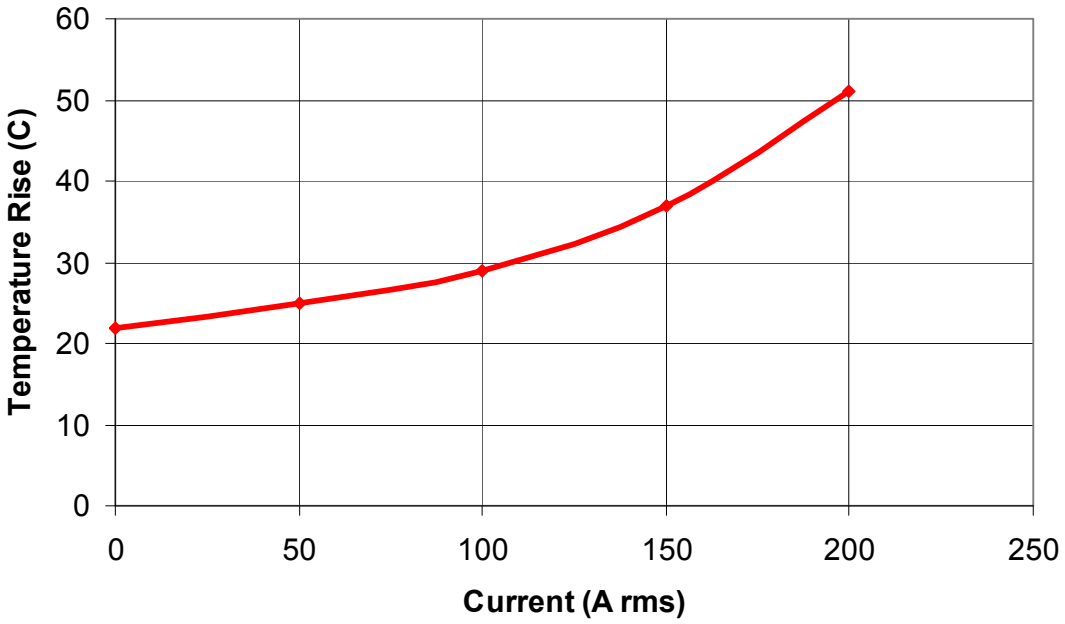

Fig. 2.36. Prius capacitor module steady-state temperature response vs. ripple current at 4 kHz.

2.1.2.3 Static capacitor test results of single sub-cell capacitor of smoothing capacitor module

The Prius and Camry capacitor modules are composed of 8 and 24 sub-cells, respectively. A sub-cell was removed from the Camry module and tested under the same test conditions that the entire module was subjected to. Since the module architecture greatly influences the overall function of the module and the difference of the number of sub-cells is significant, the most informative comparison is between the entire modules and not the sub-cells. Therefore, a comparison is not made between the Camry and Prius sub-cells; yet the Prius sub-cell capacitor test results are provided in Appendix B. Additional Camry sub-cell capacitor test results are also provided in Appendix B.

The large Camry capacitor module contains 24 86 µF sub-cell in parallel to form a total capacitance of 2098 µF; whereas the large Prius capacitor module contains (8) 141 µF sub-cell to form a total capacitance of 1,130 µF. The capacitance, ESR, and DF were measured over temperatures ranging from -40–140ºC and frequencies from 1–35 kHz and the results are shown in Figs. 2.37, 2.38, and 2.39, respectively. The capacitance increases only slightly until subjected to frequencies above 15 kHz. Figure 2.38 indicates that the ESR increases quickly with frequency at low frequencies and peaks at 5 kHz and slowly decreases with increasing frequency. Note again that the most common switching frequency of the motor and generator inverters is 5 kHz. When compared to the test results from the Prius capacitor sub-cell provided in Appendix B, the capacitance of the Camry capacitor sub-cell increases much more slowly with frequency. The ESR of the Prius capacitor sub-cell is slightly lower than that of the Camry capacitor sub-cell. The DF is much lower for the Camry capacitor sub-cell. Again, these comparisons are not straightforward as the architectural discrepancies significantly impact the overall characteristics. Nonetheless, a broad comparison of the characteristics is informative.

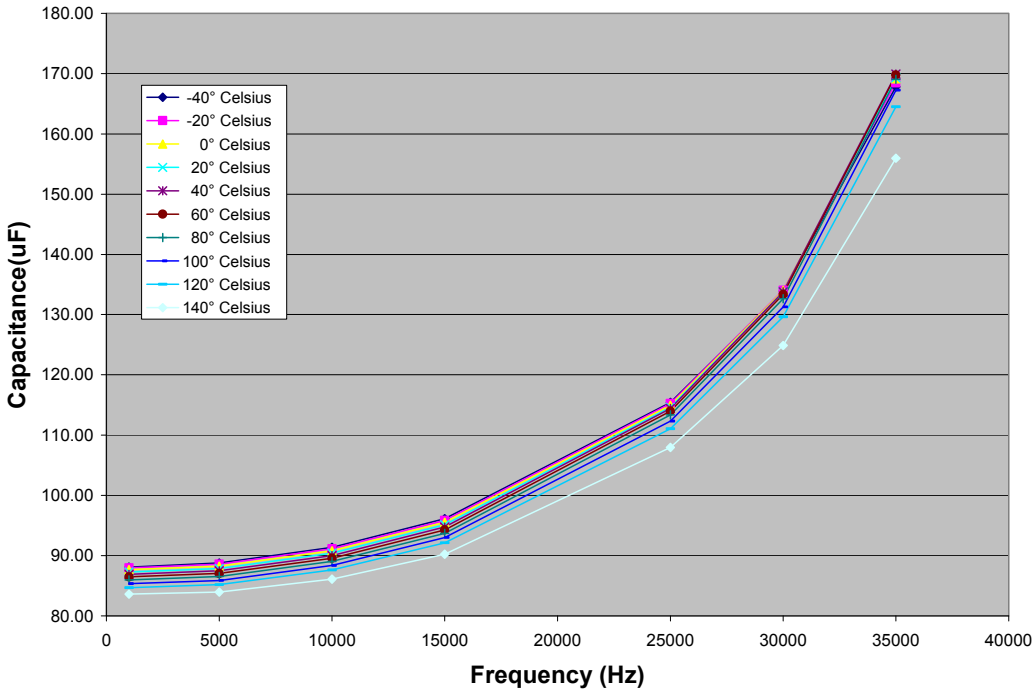

Fig. 2.37. Camry single 86 µF capacitor, capacitance vs. frequency.

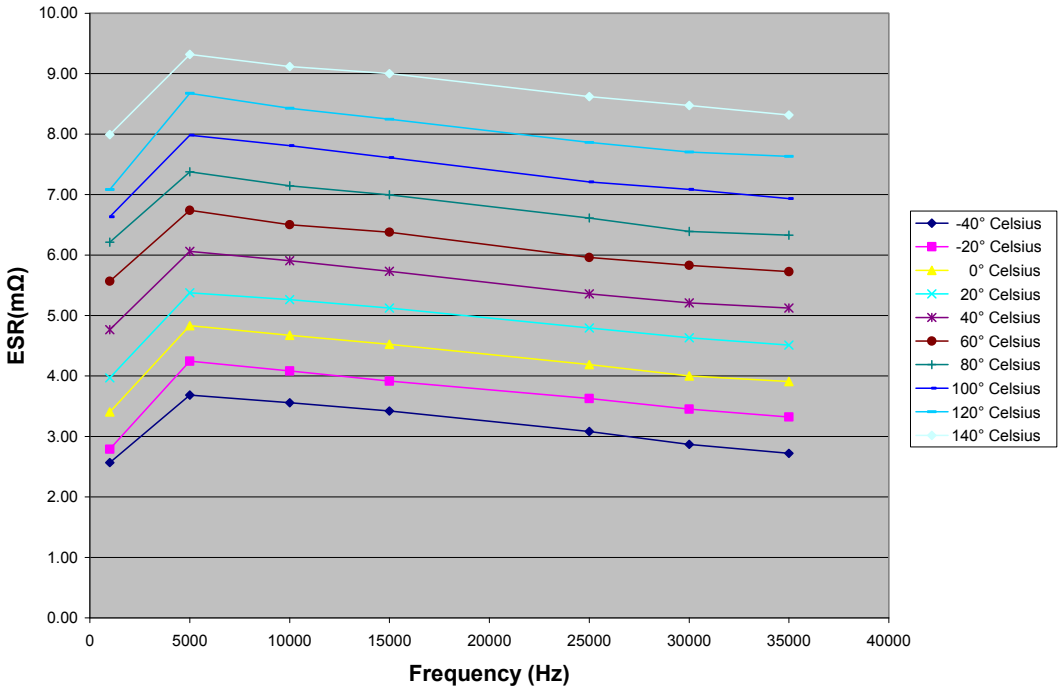

Fig. 2.38. Camry single 86 µF capacitor, ESR vs. frequency.

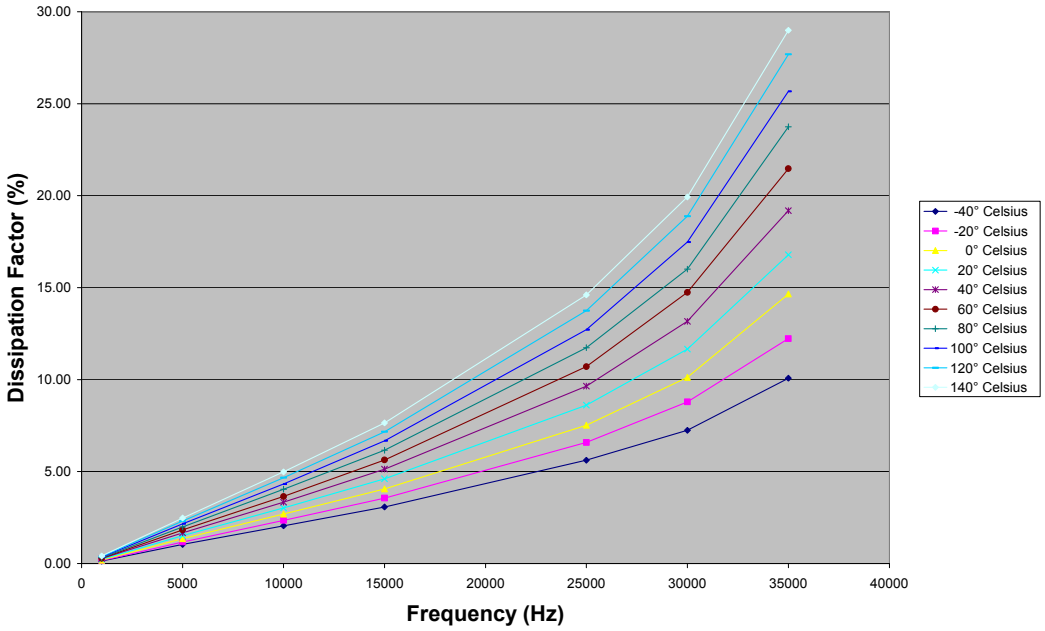

Fig. 2.39. Camry single 86 µF capacitor, DF vs. frequency.

Figures 2.40, 2.41, 2.42, and 2.43 provide the combined capacitance, ESR, and DF responses versus temperature for frequencies of 1 kHz, 5 kHz, 15 kHz, and 35 kHz, respectively. In comparing these figures, it is apparent that the high temperatures have a significant effect on the capacitance, ESR, and DF, particularly at high frequencies. Even at relatively low frequencies, the DF varies significantly with

temperature and frequency. Figures showing the results obtained while testing the Camry capacitor sub-cell at additional frequencies are provided in Appendix B. Furthermore, similar test results from the Prius capacitor sub-cell are provided in Appendix B.

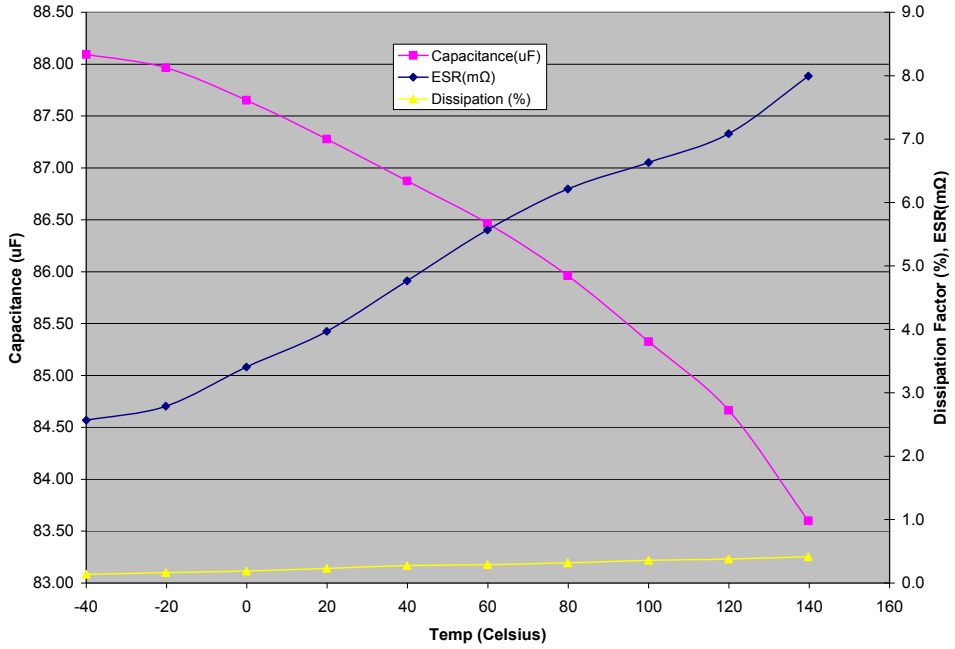

Fig. 2.40. Camry single 86 µF capacitor, capacitance, ESR, and DF vs. temperature at 1 kHz.

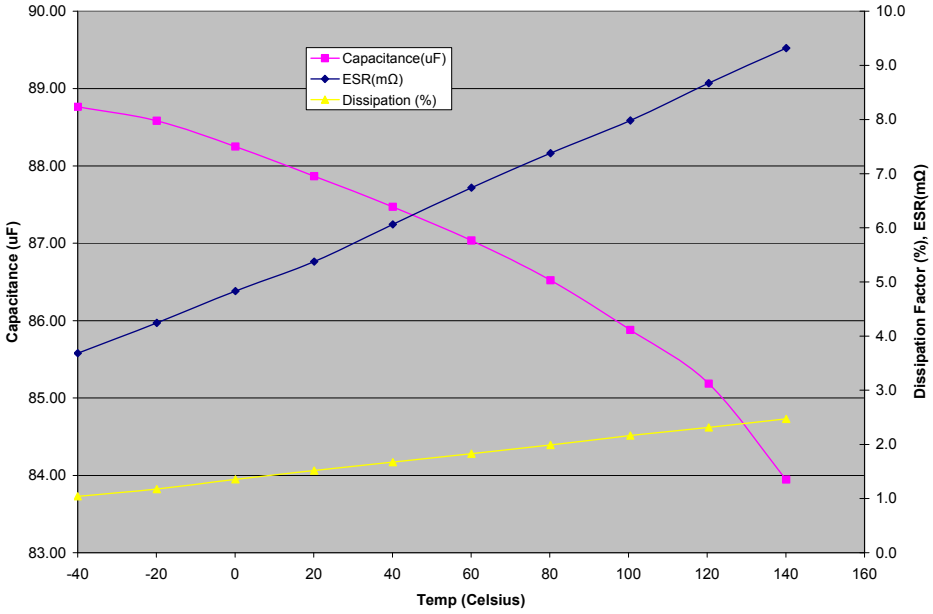

Fig. 2.41. Camry single 86 µF capacitor, capacitance, ESR, and DF vs. temperature at 5 kHz.

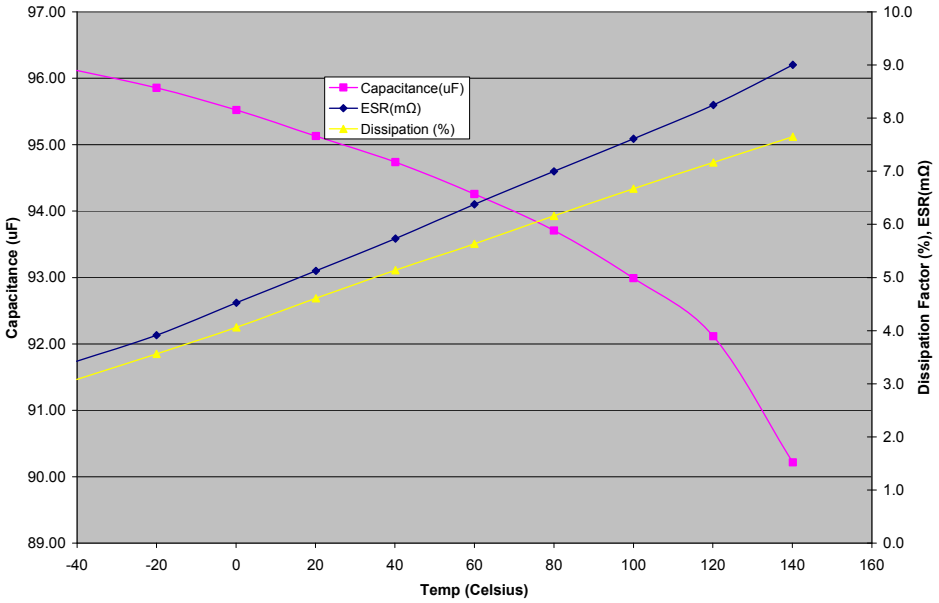

Fig. 2.42. Camry single 86 µF capacitor, capacitance, ESR, and DF vs. temperature at 15 kHz.

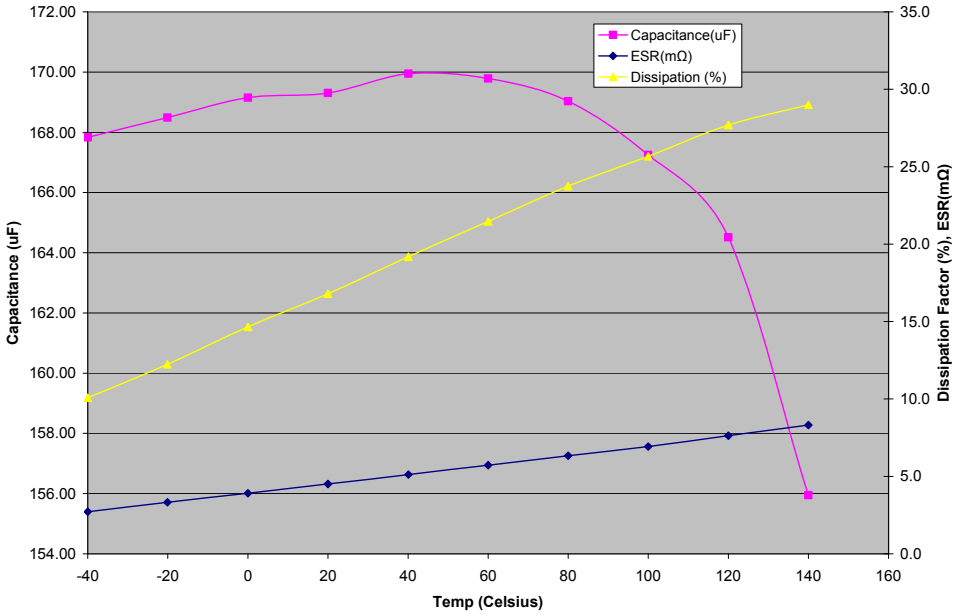

Fig. 2.43. Camry single 86 µF capacitor, capacitance, ESR, and DF vs. temperature at 35 kHz.

Figures 2.44 and 2.45 provide the combined capacitance, ESR, and DF responses versus frequency for temperatures of 20ºC and 140ºC, respectively. Although a quick comparison of the figures does not clearly reveal significant influences of temperature variation, notice the difference of scale between the figures. While the scale for capacitance remains the same, the scale for DF and ESR changes from 0–18 to 0–35 in Figs. 2.44 and 2.45, respectively. Thus, as indicated in the comparison of the previous figures, ESR and DF are significantly influenced by temperature variation. Since the unit is located within close proximity of the high operation temperatures of the ICE in addition to heat generated by components

within the PCU (including the capacitor itself), the capacitor module is often subject to high temperatures. Similar figures for the Camry and Prius capacitor sub-cells are provided in Appendix B.

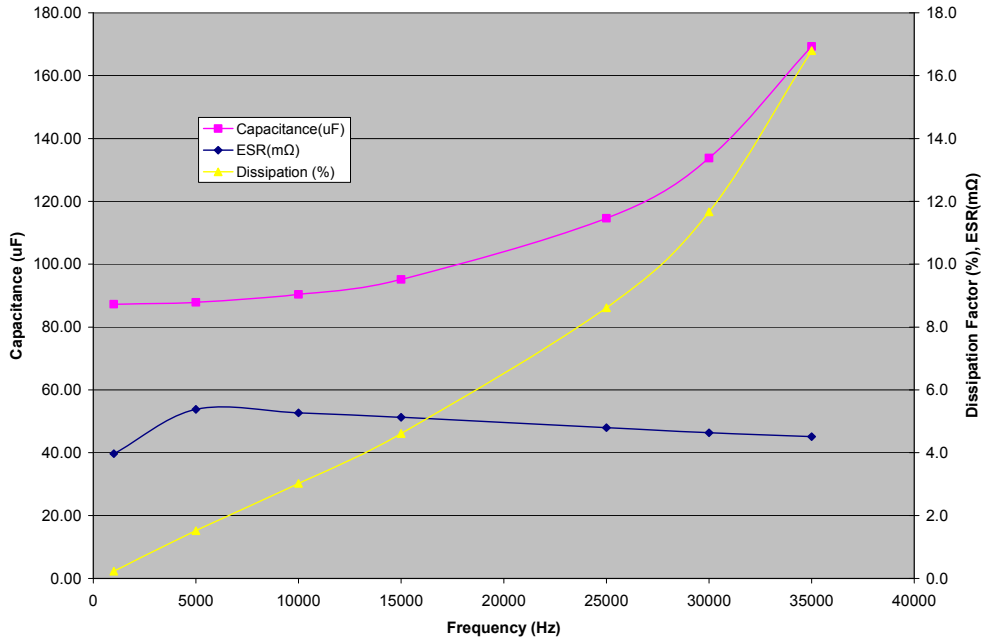

Fig. 2.44. Camry single 86 µF capacitor, capacitance, ESR, and DF vs. frequency at 20°C.

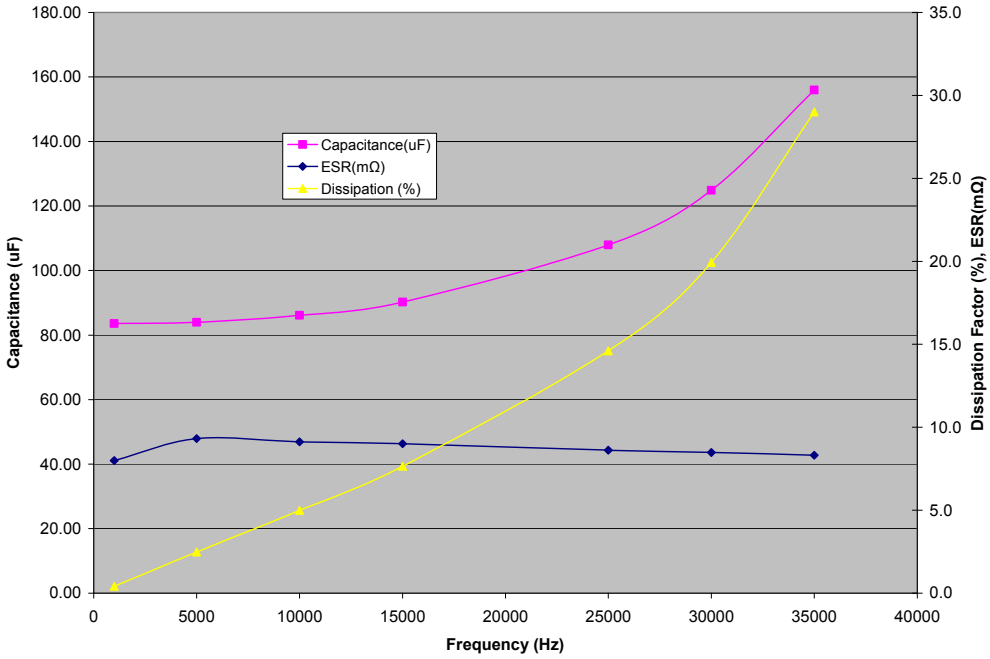

Fig. 2.45. Camry single 86 µF capacitor, capacitance, ESR, and DF vs. frequency at 140°C.

2.1.2.4 Inspection into positive reactance measurement of large dc-link capacitor module

Further inspections into the influence of frequency upon characteristics of the Camry and Prius capacitor modules were conducted using the dynamic test setup described above. A Yokogawa PZ4000 power analyzer was used to monitor the current and voltage waveforms in order to determine the respective rms values and phase differences between the two. No dc bias was applied during these tests, and all currents and voltages discussed hereon are sinusoidal in nature and the corresponding signal levels are given in terms of rms values.

The primary intent of these tests was to evaluate the voltage and current phase angle for various ripple current frequencies, as well as obtain general information regarding the voltage response of the capacitor module to a particular ripple current amplitude for various ripple current frequencies. Figures 2.46, 2.47, and 2.48 show the phase angles between the current and voltage of the Camry and Prius capacitor modules at various frequencies. These tests were conducted with about 25 A of current applied to the modules at frequencies from 5–20 kHz and all signals were measured with a Yokogawa PZ4000 wattmeter. These figures are screenshots of the Yokogawa PZ4000 measurements and they include Uac1, the rms of the ripple voltage (with no dc component), and Iac1, the rms of the ripple current, as well as the frequency, which is shown in the upper left corner of the display. The phase angle between the current and voltage was also measured, but the value is not shown in these figures. A leading phase angle is obtained when the current leads the voltage, which is typical for a capacitive reactance. A lagging phase angle is associated with an inductive reactance, in which the current lags the voltage.

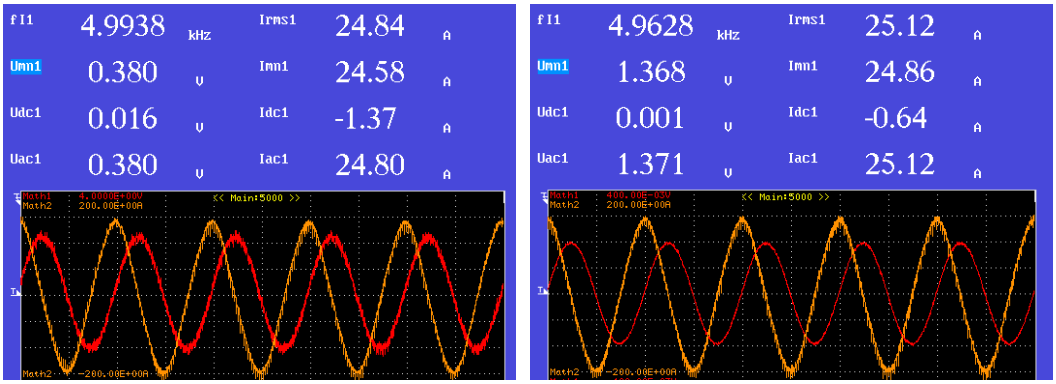

Fig. 2.46. Waveforms of the Camry (left) and Prius (right) capacitor module at 5 kHz.

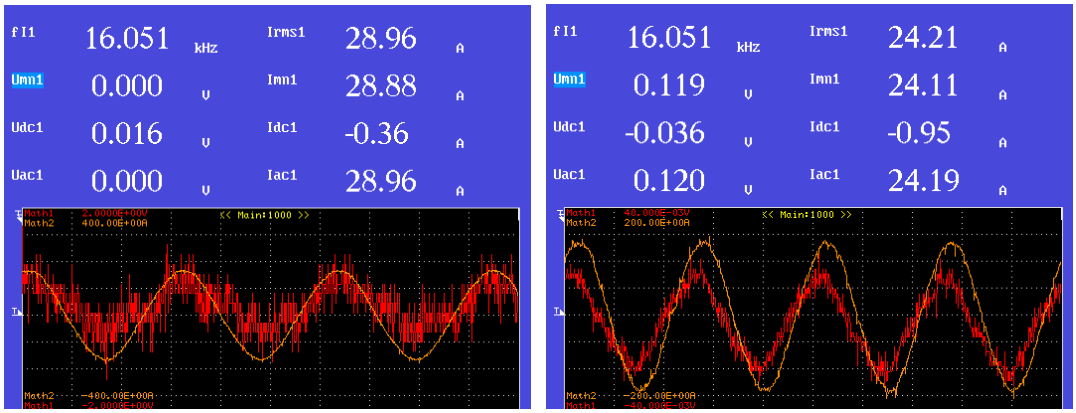

Fig. 2.47. Camry (left) and Prius (right) capacitor module waveforms at 16 kHz.

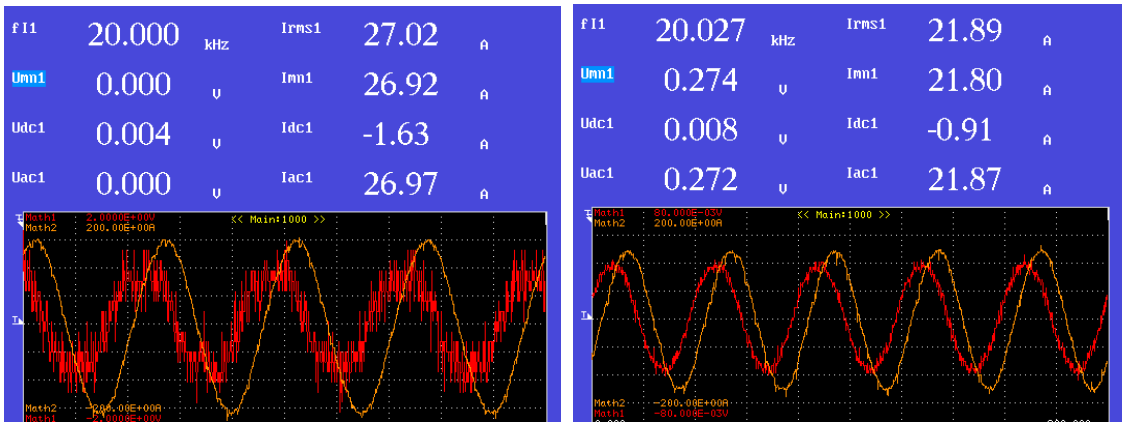

Fig. 2.48. Waveforms of the Camry (left) and Prius (right) capacitor module at 20 kHz.

Figure 2.46 shows the phase angles between the current and voltage at 5 kHz for the Camry and Prius capacitor module with the current waveform being the orange trace and having the highest amplitude. For both modules, the current is leading the voltage by an angle which is close to 90° indicating a typical capacitive response at 5 kHz. The voltage ripple of the Prius module at 25 A is higher than that of the Camry module as the capacitance of the Camry is higher than that of the Prius at this frequency.

Figure 2.47 shows screenshots obtained during a similar test with a frequency of 16 kHz for the Camry and Prius capacitor modules. The voltage waveforms contain significant noise levels as the amplitude is very low for these frequencies. The phase angle between the voltage and current of the Camry module at 16 kHz is nearly zero, and the current is lagging the voltage of the Prius module at 16 kHz indicating that the reactance is positive and the module behaves like an inductor at this frequency.

In Fig. 2.48, the frequency of the ripple current applied to both modules is 20 kHz. The phase difference between the current and voltage is large enough to easily concur that the current is lagging the voltage significantly.

A second series of tests were conducted with the Camry and Prius capacitor modules. The overall test procedures were similar to those just discussed, yet the amplitude of the signal generator (shown in Fig. 2.33) waveform was kept constant. Conditions were similar but not identical between the tests on the Camry and Prius capacitor modules and a comparison of the test results provides only general information regarding the frequencies at which the resonance and phase angle changes occur.

Figures 2.49 and 2.50 compare the responses of the Camry and Prius capacitor modules to various frequencies. In Fig. 2.49, as the applied frequency on the Camry module increases from 1 kHz, the current increases and peaks at a frequency of about 2 kHz. A similar characteristic is noticed for the Prius module and the current peaks between 2 and 3 kHz. As indicated by both figures, the current leads the voltage for low frequencies indicating a dominant capacitive effect until a frequency of about 16 kHz for the Camry and 15 kHz for the Prius. Leading phase measurements are indicated by the yellow traces, which end just prior to these resonance frequencies where the capacitive and inductive effects are equal and the corresponding reactance is zero. As the frequency increases beyond the resonant frequency, the module behaves as an inductive load as the parasitic inductance has a greater effect on the reactance than the capacitance does, even though the parasitic inductance is very low. These characteristics re-affirm that the large dc-link capacitor is used for smoothing of low machine level ripple frequencies associated with the operation the motor and generator, as opposed to being used primarily for attenuation of switching transients.

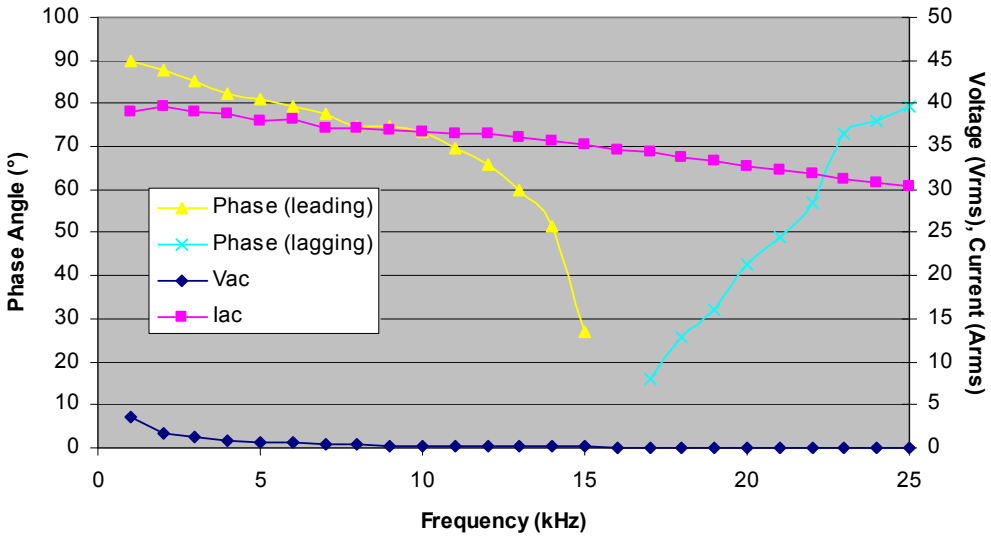

Fig. 2.49. Camry capacitor module voltage and current response to frequency.

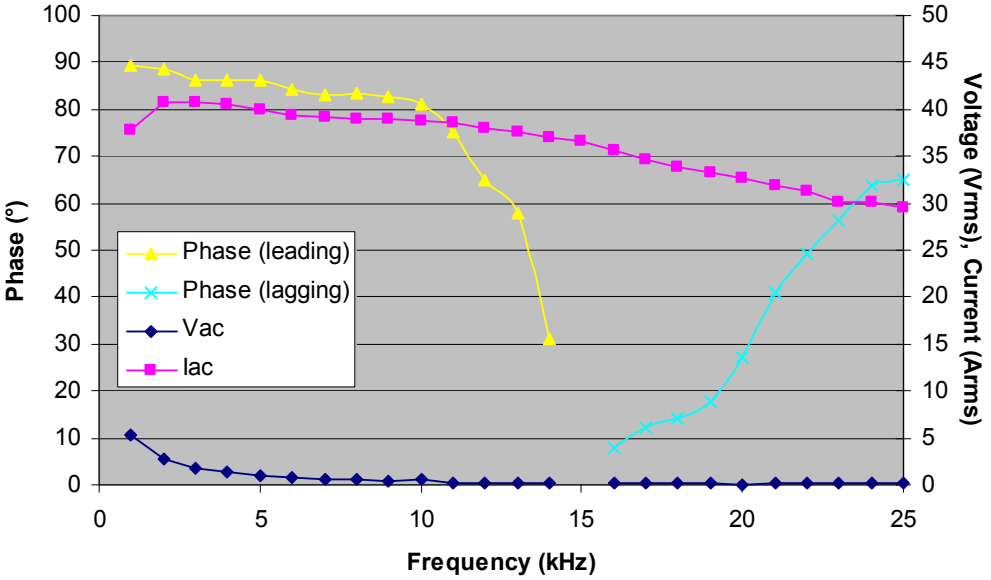

Fig. 2.50. Prius capacitor module voltage and current response to frequency.

2.1.2.5 Static capacitor test results of battery level filter capacitor evaluations

Figures 2.51 and 2.52 compare the capacitor test results of the 500 V, 378 µF capacitor of the Camry and the 600V, 282 µF capacitor of the Prius, respectively. Each capacitor resides between the battery and the boost converter and is located within the PCU. Significant differences are noticed between the characteristics of the two capacitors, particular when comparing the influence of frequency upon capacitance and DF. The equivalent capacitance of the Prius begins to approach infinity near about 22 kHz, whereas the equivalent capacitance of the Camry capacitor only increased slightly as the maximum test frequency of 30 kHz was reached. Since DF is a product of ESR, capacitance, and frequency, the DF curves have characteristics similar to those of the capacitance curves.

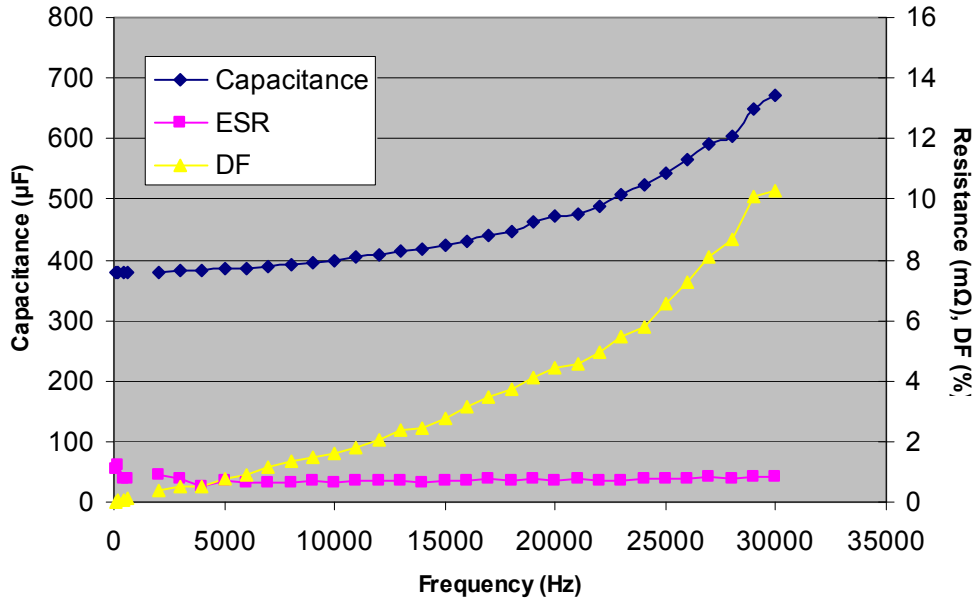

Fig. 2.51. Camry battery level 378 µF capacitor, capacitance, ESR, and DF vs. frequency.

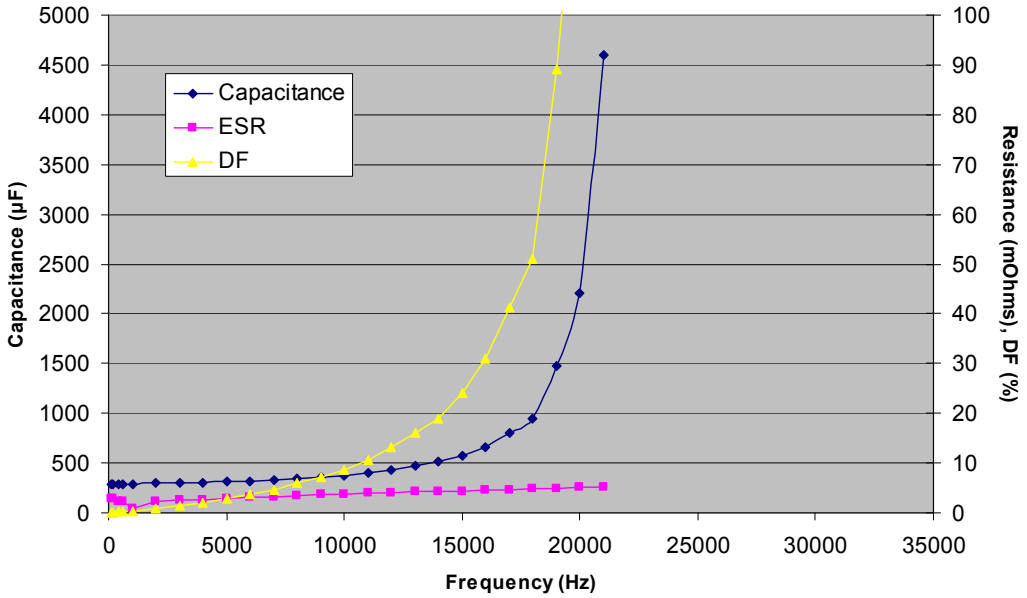

Fig. 2.52. Prius battery level 282 µF capacitor, capacitance, ESR, and DF vs. frequency.

2.1.2.6 Static capacitor test results of small dc-link capacitor evaluations

Figures 2.53 and 2.54 compare the capacitor test results of the dc-link 750 V, 0.9 µF capacitor of the Camry and the 750V, 0.1 µF capacitor of the Prius, respectively. Although the equivalent capacitance of the small Camry capacitor appears to decrease significantly, a closer look at the capacitance axis limits indicates that frequency has a small effect on the equivalent capacitance of the small Camry and Prius capacitors. Unlike the ESR of the other capacitors, the ESR of both small capacitors is much higher for

low frequencies and decreases quickly with increasing frequency. All data points were taken at room temperature. The DF is relatively low even at high frequencies. These characteristics indicate the high frequency filtering capabilities of the small capacitors.

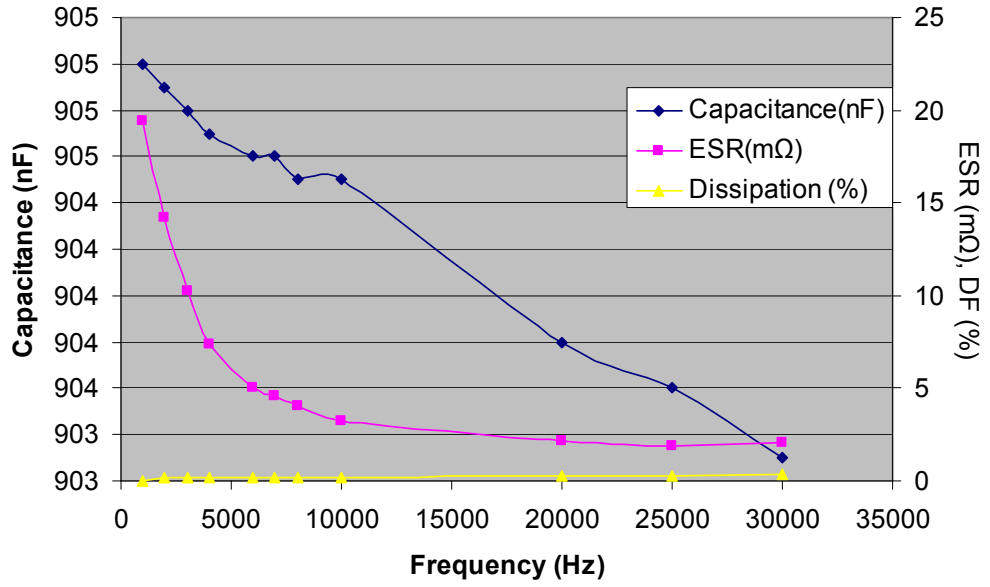

Fig. 2.53. Camry dc-link 0.9 µF capacitor, capacitance, ESR, and DF vs. frequency.

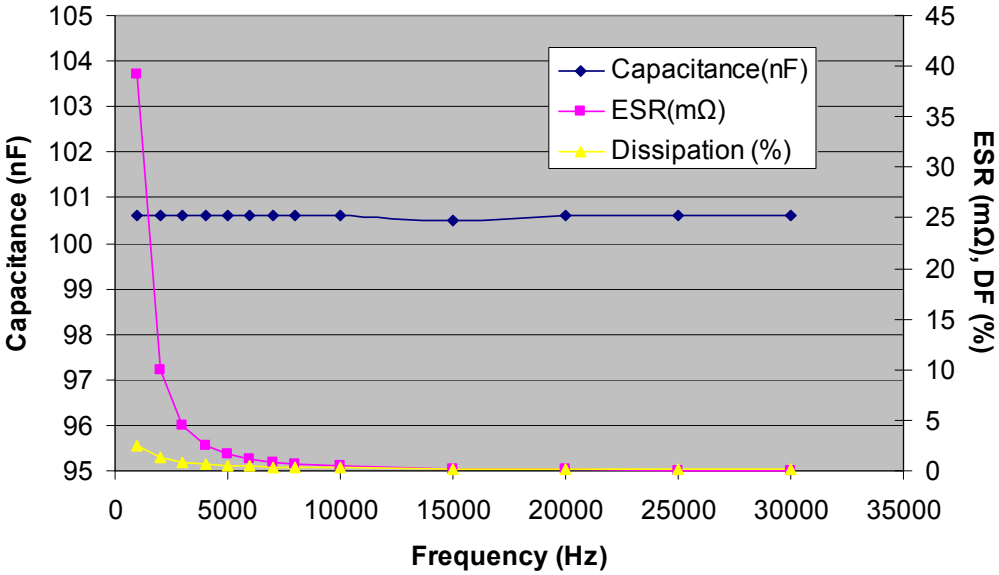

Fig. 2.54. Prius dc-link 0.1 µF capacitor, capacitance, ESR, and DF vs. frequency.

2.2 TRANSAXLE

The 2007 hybrid Camry transaxle assembly is comprised of motor, generator, and gear box subassemblies. The mass of the entire unit is 108 kg, which is shown in Fig. 2.55. An ICE mounts to the transaxle and a mechanical interface is established with spline shaft, which is slightly visible in the figure.

The electric motor and generator outputs are not directly accessible yet through a combination of various gear configurations, the total motive force output of the hybrid system is supplied to the drive shafts by the differential gear outputs which are indicated in the figure. The generator is located adjacent to the ICE input (referred to as front end) and the motor is located in the rear portion of the transaxle, as shown in Fig. 2.56. The gear section of the transaxle is located between the generator and motor sections, as shown in Fig. 2.57.

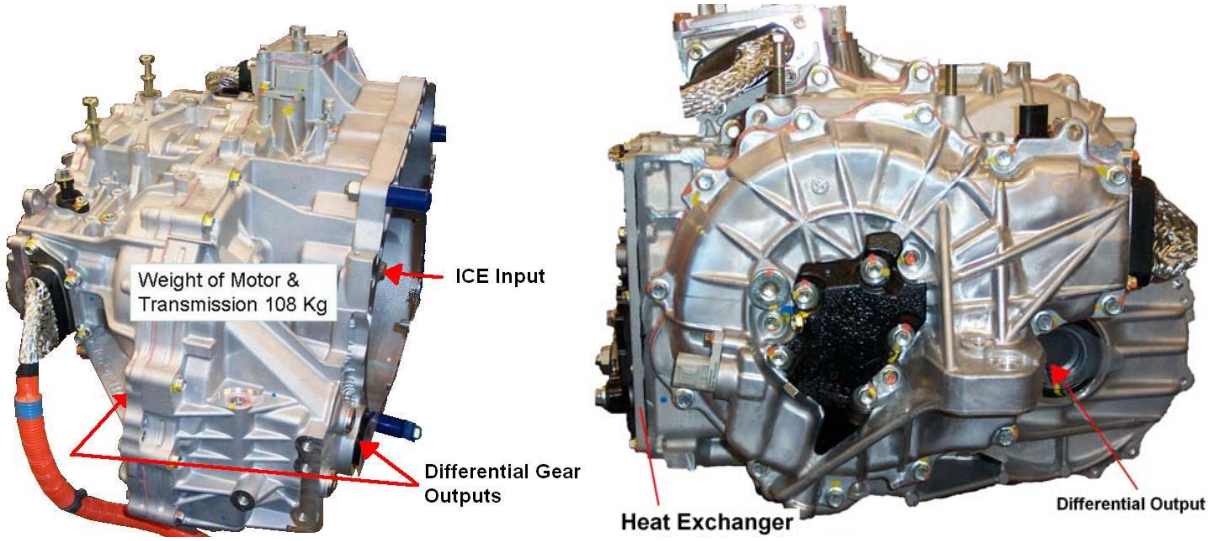

Fig. 2.55. Hybrid Camry transaxle isometric view (left) and rear view (right).

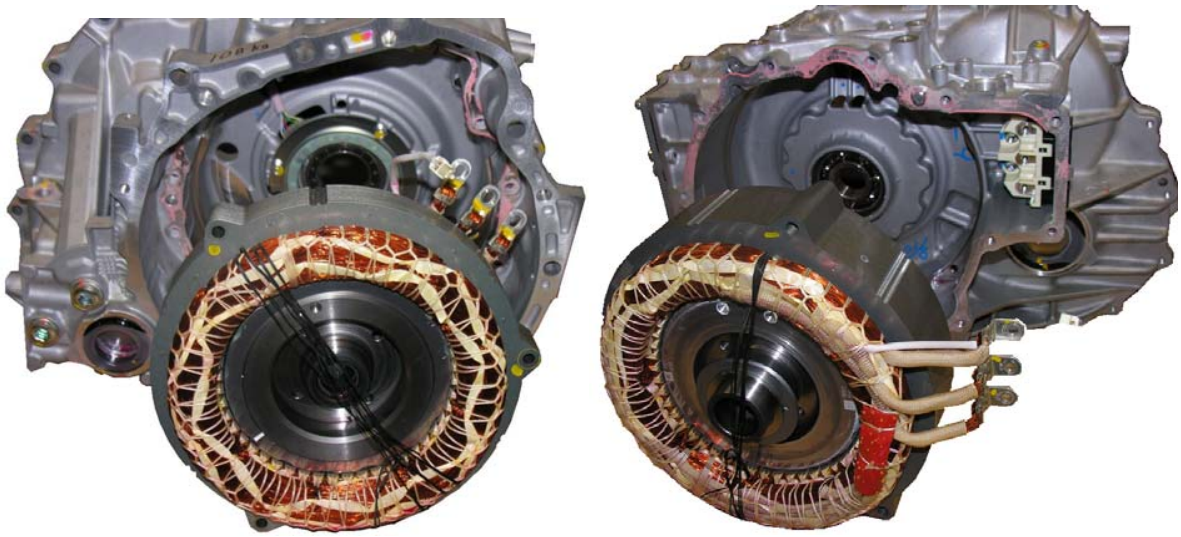

Fig. 2.56. Camry generator front view with ICE spline removed (left) and motor rear view (right).

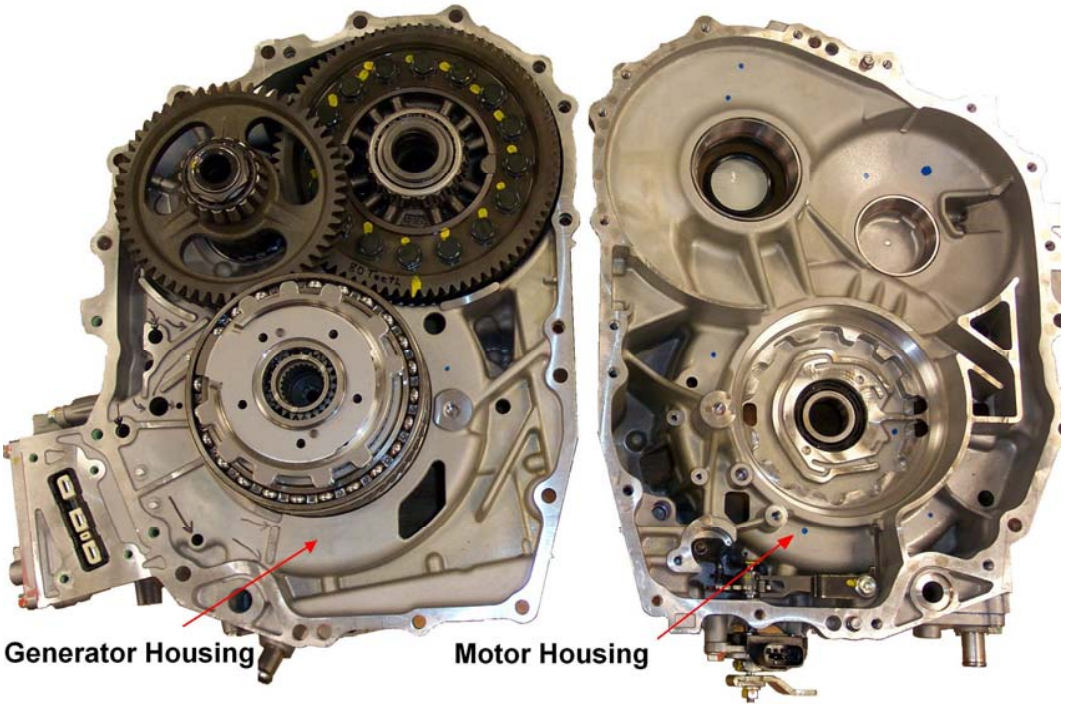

Fig. 2.57. Camry transaxle gear section open sandwich view.

2.2.1 Thermal Management and Lubrication System

The thermal management and lubrication system of the transaxle utilizes a mechanically driven trochoid oil pump as well as oil slinging movement by the drive gears to circulate oil throughout the transaxle. As shown in Fig. 2.58, the trochoid shaft is driven by the planetary carrier, which is connected directly to and rotates at the same speed as the ICE. The black plate was removed from the rear of the trochoid system to provide a view of the interior of the trochoid pump. An oil pickup is located near the bottom of the motor section which serves as an input to the trochoid pump. The central component of the trochoid pump resembles a gear and is machined such that the oil collects in the gaps of the pump teeth and forces the oil through the trochoid shaft shortly thereafter. The motor rotor shaft is hollow and the trochoid pump shaft extends through the hollow shaft of the motor rotor. A portion of the oil is dispensed to the motor bearing which is located next to the toothed central component of the trochoid pump. Small holes are located along the side of the trochoid pump shaft to supply oil to another motor bearing on the opposite end of the motor rotor. The tip of the trochoid pump shaft supplies oil to the power split and speed reduction gear through the same interface in which the shaft is driven. The 2004 Prius contains a similar trochoid pump mechanism.

Note that oil is not circulated by the trochoid pump if the ICE is not active. Therefore, if the vehicle is operating in electric mode only, then the system fully depends on the oil slinging action of the gear train for oil circulation. A general diagram of the oil flow paths is provided in Fig. 2.59. Oil that has settled in the bottom portion of the gear section is picked up by the differential gear teeth and is then slung to the driver gear, to reservoirs in the upper portion of the gear section, and to the power split planetary gear unit. The oil reservoirs are flooded if the differential gear is rotating above 900 rpm. A large reservoir is adjacent to a heat exchanger in order to transfer heat to the cooling system. Weep holes and oil ports distribute oil to the motor and generator stator as well as several bearings throughout the system. Note that the circulation due to gear slinging is dependent upon vehicle speed.

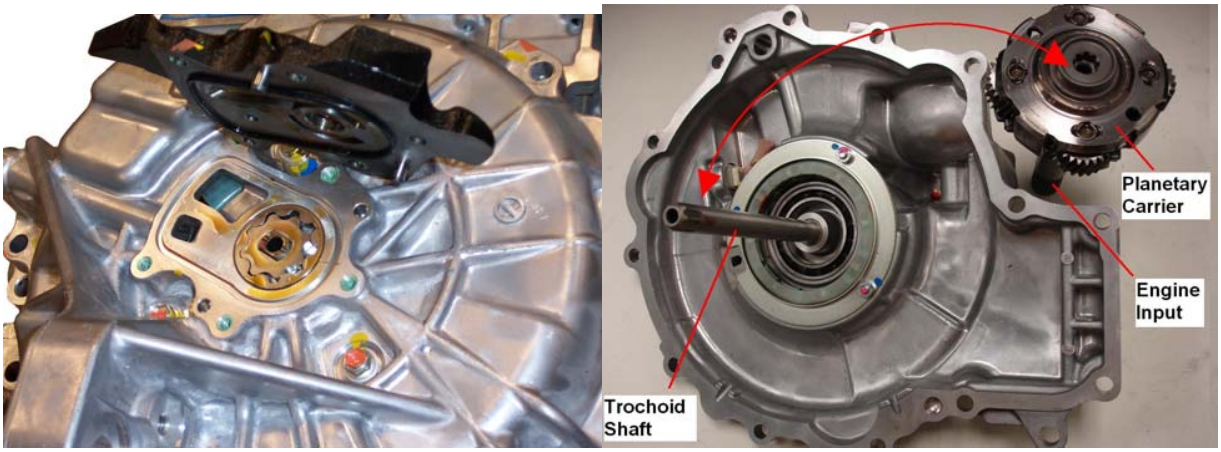

Fig. 2.58. Trochoid oil pump view from outside rear (left) and from inside motor section (right).

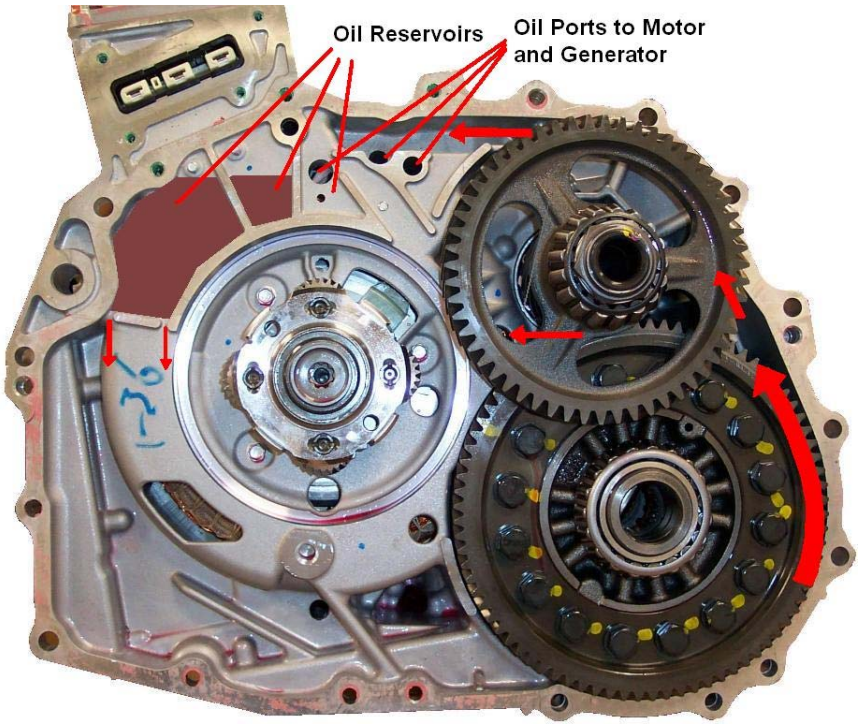

Fig. 2.59. Oil slinging paths formed by gear train.

A heat exchanger is located on the one side of the motor periphery and the generator also has a small heat exchanger which is part of a series coolant loop with the motor heat exchanger as well as the PCU heat exchanger. According to specifications in the Camry repair manual, the coolant loop consists of a standard 50% ethlyene glycol and 50% water mixture which flows at 10 L per minute and has an average operation temperature of 65ºC. Vehicle tests at Argonne National Laboratory (ANL) indicate the average coolant temperature may be considerably lower depending on operation conditions. The coolant capacity is listed as 2.9 L. A separate radiator is dedicated to the THS coolant loop which is isolated from the ICE coolant loop that operates at much higher temperatures.

2.2.2 Transaxle Gear Train

The Camry transaxle has three primary gear systems which are designed to carry out power split, speed reduction, and drive functions. A general comparison of the 2004 Prius gear train and the 2007 Camry gear train is provided in Fig. 2.60. The number of teeth on each gear is noted in black text on a white background. There are several noticeable differences between the two designs. The Prius transaxle design has a chain coupling between the power split planetary ring and the counter drive gear, whereas the planetary ring and counter drive gears mesh directly within the Camry transaxle. Additionally, the Camry transaxle has only three separate axes about which gear systems rotate, compared to four axes in the Prius transaxle. The number of teeth on the planetary gear components does not differ between the two designs. The total gear ratio from the Camry power split planetary ring to the differential output is $(80/23) \times (55/54) = 3.542$, where the equivalent gear ratio for the Prius is $(75/26) \times (44/30) \times (35/36) = 4.113$.

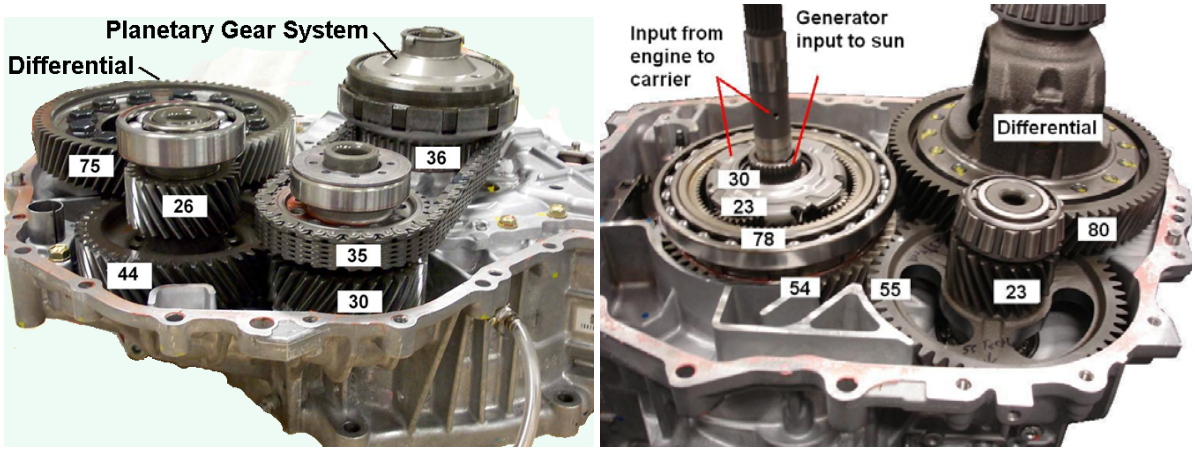

Fig. 2.60. 2004 Prius gear train (left) and 2007 Camry gear train (right).

Another significant difference between the designs is that the Camry has a speed reduction gear, which is comprised of a planetary gear unit. The speed reduction planetary gear assembly is shown along with the power split planetary gear unit in Fig. 2.61. The planetary gear units share the ring gear in which the electric motor, MG2, is connected to the ring gear through the speed reduction gears. The number of teeth is shown for each gear and the planetary carrier is fixed to the chassis. Thus, the gear ratio between the electric motor shaft is $(57/18) \times (18/23) = 2.478$, where the MG2 spins 2.478 times faster than the ring gear and therefore the torque output of MG2 is effectively multiplied by 2.478 prior to reaching the ring gear. Gear teeth on the outer periphery of the ring gear, collectively referred to as the counter drive gear, mesh with the counter driven gear which supplies motive force to the drive shafts though the final and differential gear units. Consequently, the speed of MG2 is directly proportional to the speed of the vehicle. The generator rotor shaft is hollow and connects to the sun gear of power split planetary and the input shaft from the ICE is fed through the hollow generator shaft and connects to the planetary carrier. A locking gear mechanism is adjacent to the counter drive gear which is engaged when the vehicle gear selector is placed in park. A summary of the number of gear teeth for each gear is provided in Table 2.6. Since the Prius drive gear train is moderately different from the Camry drive train, a comparison is not easily made between each component of the drive train, but is more meaningful if the overall gear ratio is compared, as provided previously.

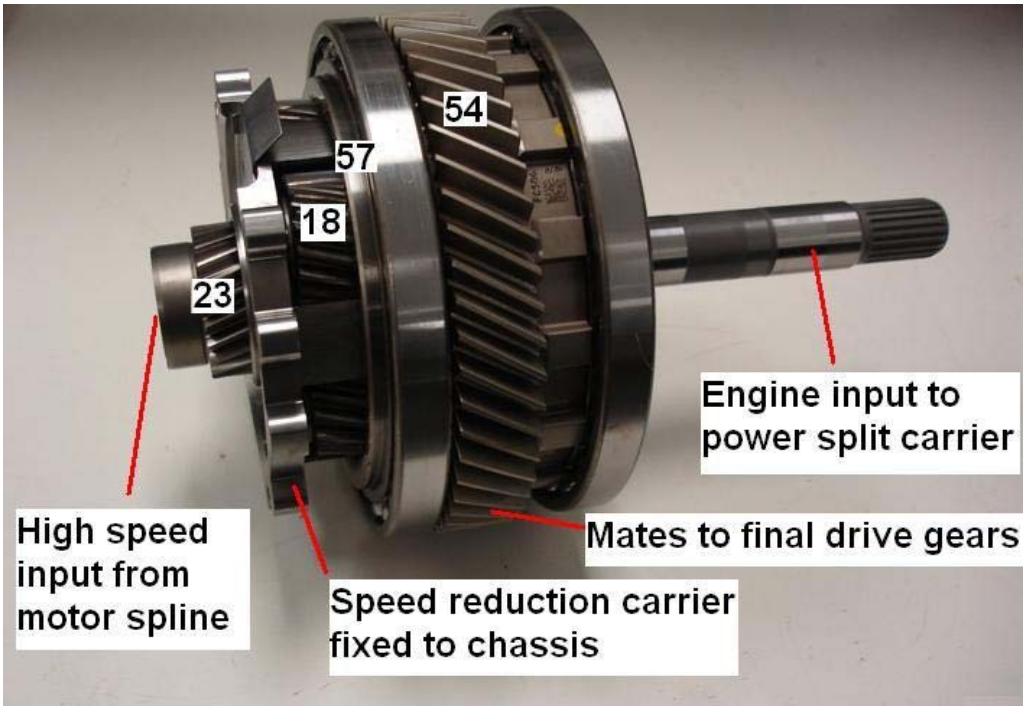

Fig. 2.61. Camry speed reduction planetary and power split planetary.

Table 2.6. Camry transaxle gear information

Power Split Planetary Gear Unit	The No. of Ring Gear Teeth		78	
	The No. of Pinion Gear Teeth		23	
	The No. of Sun Gear Teeth		30	
Motor Speed Reduction Planetary Gear Unit	The No. of Ring Gear Teeth		57	
	The No. of Pinion Gear Teeth		18	
	The No. of Sun Gear Teeth		23	
Counter Gears	The No. of Drive Gear Teeth		54	
	The No. of Driven Gear Teeth		55	
Final Gears	The No. of Drive Gear Teeth		23	
	The No. of Driven Gear Teeth		80	
Total Deceleration Ratio			3.542	

2.2.3 Motor Mass and Volumetric Assessments

When comparing the Camry and Prius electric drive characteristics, the mass and volume of the primary electric drive motor, MG2, was decreased although the peak and continuous power capabilities of the motor increased. This was primarily accomplished by increasing the rated speed of the motor from about

6,000–14,000 rpm. To clarify the benefit of increasing the speed rating, the torque and power rating of the Prius motor is given in Fig. 2.62. These are shown to present the general speed, torque, and power relationship of any motor as power is equal to torque times speed. Therefore, a much lower torque is required to produce a certain power level at a higher speed than for a lower speed. For example, a torque of 382 Nm is required to produce 40 kW at 1000 rpm, whereas only 38.2 Nm is required to produce 40 kW at 10,000 rpm. Additionally, torque is proportional to current and, roughly speaking, the amount of current required to produce a consistent power level decreases with increasing speed. While this is not entirely an accurate statement as there are many factors to consider when making such a comparison, the concept generally holds true.

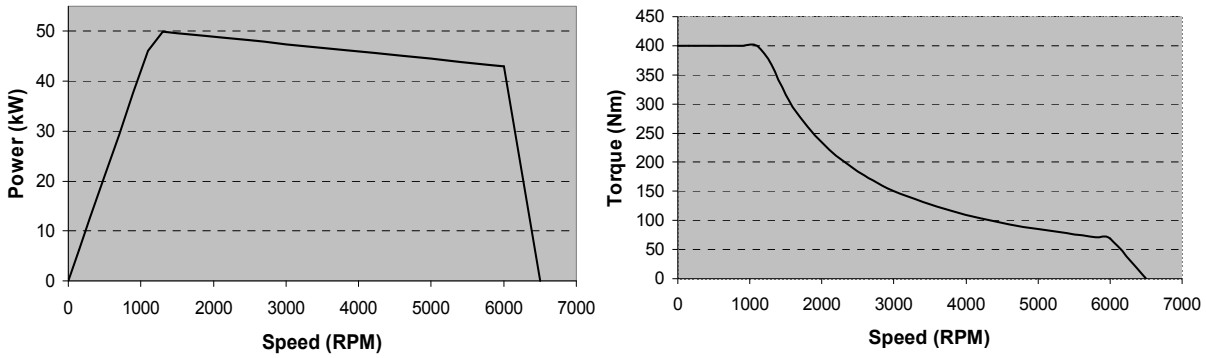

Fig. 2.62. Speed, torque, and power relationship.

There are a few negative aspects of moving to higher motor speed ratings however. Typically, the low speed torque rating of the motor is compromised when the speed rating is increased. Therefore, the lowest speed at which rated power can be developed, namely base speed, increases. Again, these relationships depend upon various motor design parameters such as rotor diameter, lamination stack length, magnet strength, and winding configuration, yet these relationships are typically pertinent. As rotor speed ratings increase, additional mechanical design aspects must be considered. Improved support must be provided by the rotor laminations to retain the PMs which are subjected to forces which are directly proportion to the square of the rotor speed. Additionally, bearings must be designed to withstand the high speeds of the rotor shaft. Depending on the characteristics of the PMs, rotor, and stator, core losses and induced back-emf voltages typically increase with increasing rotor speed. The high speed reduction gear used in the Camry design is required to convert the high speed of the motor to properly match the remaining transaxle design. Although the torque rating of the Camry is only 270 Nm, the maximum torque is converted to about 670 Nm through the speed reduction gear.

Figures 2.63 and 2.64 provide various views of the Camry transaxle and the volume associated with the primary drive motor. Certain key dimensions are shown, but several others are needed to determine volume since the motor terminal box, and especially the heat exchanger shown in Fig. 2.64 have complex geometries. Since the motor casing also houses some of the gear box, the motor casing had to be well defined to arrive at the mass and volume, excluding areas unrelated to the motor. For example, in Figs. 2.63(a) and 2.63(b), the surface chosen for the end of the motor housing is indicated.

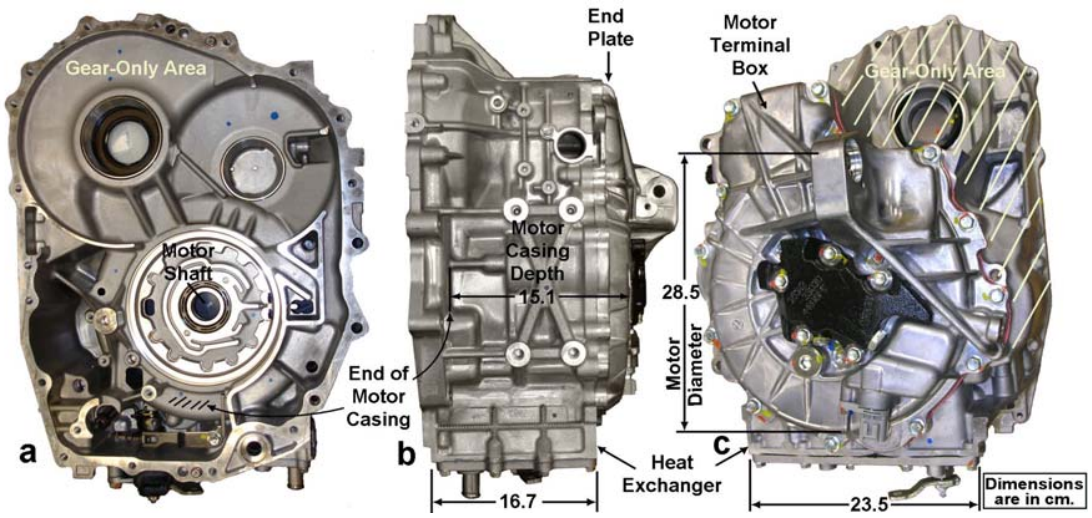

Fig. 2.63. Camry motor assembly after separation from generator assembly.

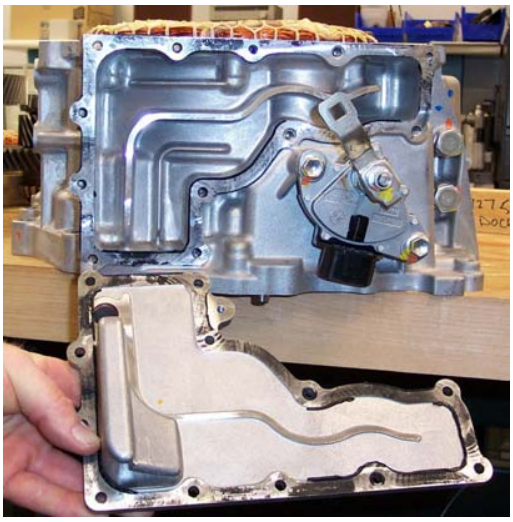

Fig. 2.64. Coolant channel at bottom of motor casing.

The results of the packaging assessment were used to generate estimates of peak specific power and peak power density as summarized and compared to the Prius specs in Table 2.7. Because of advantages gained by increasing the maximum speed from 6,000–14,000 rpm, Toyota was able to optimize the Camry design such that motor volume and mass were both lower than for the Prius in spite of a higher published peak power rating. It is appropriate to include the mass and volume of the Camry speed reduction planetary gear in this comparison with the Prius and doing so mitigates the perceived improvement upon the Prius design.

Table 2.7. Specific power and power density estimates for the PMSM

Parameter	Camry	Prius
Motor peak specific power (without converter), kW/kg	70/~41.7 = **~1.68**	50/45.0 = **1.11**
Motor peak power density, kW/L	70/~14.8 = **~4.73**	50/15.4 = **3.25**

Figure 2.65 shows the stator assembly that was removed from the Camry transaxle assembly. The entire Camry stator assembly mass is 18.0 kg, whereas the Prius stator assembly mass is 25.9 kg, with 5.7 kg and 6.8 kg of copper within each stator, respectively. The three-phase power input ("output" during regenerative braking) leads are clearly evident. A thermistor is embedded in the stator windings and the corresponding leads are routed adjacently to the motor leads. There are 18 wires bundled in each motor lead which splits in half to form a parallel winding configuration. The Camry stator windings have 9 strands of copper with 14 turns per pole and the Prius stator windings have 13 stands of copper with 9 turns per pole in parallel and series configurations, respectively. Notice that the product of the number of strands and the number of turns has a comparable result between the Camry and the Prius.

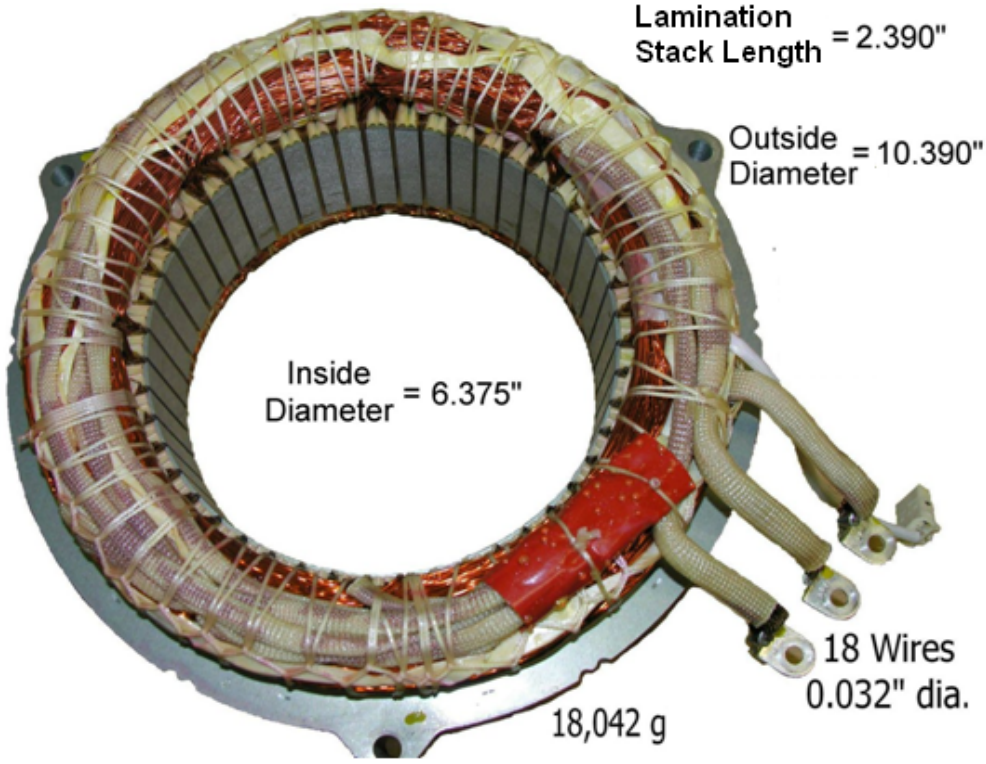

Fig. 2.65. Camry motor stator.

A comparison of the Camry and Prius laminations is provided in Fig. 2.66. In Fig. 2.66(a), a Camry motor stator lamination is placed on top of a Prius motor stator lamination, showing that the outer diameter (OD) of the Camry lamination is slightly smaller than that of the Prius. Through both Figs. 2.66(a) and 2.66(b) it is shown that the Camry motor stator slots are somewhat shorter, yet they are wider than the slots on the Prius motor stator laminations. The Camry generator stator laminations are identical to the Camry motor stator laminations. The motor lamination stack thickness has reduced from 3.29" on the Prius to 2.39" on the Camry. The Camry generator lamination stack thickness is 1.41". The inner diameters (IDs) of the Camry motor, Camry generator, and Prius motor stator laminations are equal. The stack lengths and outer diameters of the rotors have corresponding similarities.